ELSEVIER

Chemical Geology 225 (2006) 121–136

CHEMICAL GEOLOGY
INCLUDING
ISOTOPE GEOSCIENCE

www.elsevier.com/locate/chemgeo

Determination of mass-dependent molybdenum isotopic variations by MC-ICP-MS: An evaluation of matrix effects

Aaron J. Pietruszka [a,b,*], Richard J. Walker [b], Philip A. Candela [b]

[a] *Department of Geological Sciences, San Diego State University, 5500 Campanile Drive, San Diego, CA 92182-1020, USA*
[b] *Department of Geology, University of Maryland, College Park, MD 20742, USA*

Received 27 March 2005; received in revised form 19 September 2005; accepted 26 September 2005

Abstract

Several analytical techniques are currently used to determine mass-dependent molybdenum isotopic variations in natural materials using multiple-collector inductively coupled plasma mass spectrometry (MC-ICP-MS), including different methods for the separation of Mo from the sample and the correction for instrumental mass-dependent isotopic fractionation (instrumental mass bias). Both internal ("double-spiking" using two enriched Mo isotopes) and external ("zirconium doping" with standard-sample bracketing) techniques have been used in previous studies to deal with the effects of instrumental mass bias. The results of these studies have indicated that the precision for Mo isotopic analyses of natural (matrix-bearing) samples is a factor of ~4–7× better using a double spike. Here we present a detailed study of the ability of MC-ICP-MS to determine, both precisely and accurately, the isotopic composition of Mo extracted from molybdenite using a low blank, high yield two-column procedure for Mo separation and a simple standard-sample bracketing approach to correct for instrumental mass bias. Based on analyses of molybdenites, the precision of this technique is shown to be similar to published double-spike data (within a factor of ~2). All three of the known types of potential matrix effects in the MC-ICP-MS are also evaluated: automatrix effects, matrix effects due to Zr doping and matrix effects due to elements in the sample other than Mo and Zr. Each of these matrix effects is found to be either insignificant or controllable. Analyses of five molybdenites of hydrothermal origin reveal a range in their Mo isotopic composition that is a factor of ~4 greater than the previous range reported for such samples. More detailed work is required to elucidate the origin of these mass-dependent Mo isotopic variations in molybdenites.

Keywords: Molybdenum; Isotopes; Mass spectrometry; Plasma ionization; MC-ICP-MS; Matrix effects; Molybdenite

1. Introduction

High-precision isotopic measurements of several "heavy" elements, such as iron (e.g., Beard and Johnson, 1999; Zhu et al., 2000a; Walczyk and von Blanckenburg, 2002; Beard et al., 2003; Kehm et al., 2003; Matthews et al., 2004), copper (e.g., Maréchal et al., 1999; Zhu et al., 2000b), selenium (e.g., Rouxel et al., 2002; Ellis et al., 2003), molybdenum (e.g., Anbar et al., 2001; Barling et al., 2001; Siebert et al., 2001, 2003, 2005; McManus et al., 2002; Nägler et al., 2005), cadmium (e.g., Wombacher et al., 2003), antimony (e.g., Rouxel et al., 2003) and thallium (e.g., Rehkämper et al., 2002), in geological and biological materials have revealed small, but significant, mass-dependent variations due to a wide range of natural processes. Although some of these studies (e.g., Beard and John-

* Corresponding author. Department of Geological Sciences, San Diego State University, 5500 Campanile Drive, San Diego, CA 92182-1020, USA. Tel.: +1 619 594 2648; fax: +1 619 594 4372.
E-mail address: apietrus@geology.sdsu.edu (A.J. Pietruszka).

0009-2541/$ - see front matter © 2005 Elsevier B.V. All rights reserved.
doi:10.1016/j.chemgeo.2005.09.002

son, 1999; Ellis et al., 2003) have relied upon thermal ionization mass spectrometry (TIMS), the recent development of the multiple-collector inductively coupled plasma mass spectrometer (MC-ICP-MS) has made it possible to conduct these measurements to a higher degree of precision and efficiency than was previously possible (e.g., Halliday et al., 1998). The main advantage of MC-ICP-MS for these types of analyses, compared to previous techniques using TIMS, are typically noted to derive from two factors (e.g., Albarède et al., 2004): (1) the nearly complete ionization of elements in the plasma source that are difficult to ionize thermally, which results in a sensitivity for such elements by MC-ICP-MS that is greater than TIMS and (2) the ability to correct the measured isotope ratios of one element for the effects of instrumental mass-dependent isotopic fractionation ("instrumental mass bias") using another element (impossible by TIMS) and/or a comparison of the measured isotope ratios of the sample and a pair of bracketing standards (difficult by TIMS).

The small magnitude of the natural fractionation between isotopes of heavy elements requires the careful evaluation and control of analytical artifacts (e.g., Albarède et al., 2004). The accuracy and precision of isotopic measurements by MC-ICP-MS depend upon a number of factors that may arise during the chemical separation and mass spectrometric analysis of an element from a natural sample. One of the greatest challenges of MC-ICP-MS measurements is the correction for instrumental mass bias. Two broad classes of techniques have been devised: (1) a simple comparison of the measured isotope ratios of the sample and a pair of bracketing standards ("standard-sample bracketing" or SSB), with or without the addition of another element as an external monitor of instrumental mass bias (e.g., "Zr doping"), or, less frequently, (2) the addition of two enriched isotopic tracers with known concentrations to the sample for a completely internal mass-bias correction ("double spiking"). Another critical task is to remove, as far as possible, all other elements from the sample (the "matrix") while maintaining a nearly complete recovery of the element of interest. The latter issue (complete recovery) is important because many studies have demonstrated that isotopic fractionation of heavy elements such as iron, copper, molybdenum or cadmium may occur during their chromatographic separation from a sample matrix (Maréchal et al., 1999; Anbar et al., 2000, 2001; Siebert et al., 2001; Maréchal and Albarède, 2002; Wombacher et al., 2003). However, it is important to note that such isotopic fractionation can be minimized if the elemental yield is nearly complete. The former issue (matrix removal) is important for several reasons. First, it is necessary to remove any elements that cause direct isobaric interferences with the isotopes of the element of interest. Second, it is necessary to remove an element that will be added to the sample later to correct for the effects of instrumental mass bias. Third, it is necessary to remove all other elements from the sample in order to prevent significant isotopic "matrix effects" in the MC-ICP-MS (e.g., Carlson et al., 2001). Matrix effects may also arise during mass spectrometry due to variations in the relative concentration of the element in the sample and bracketing standard ("automatrix" effects) or due to variations in the relative concentration of the element of interest and the normalizing element.

Previous studies have shown that molybdenum displays significant, and systematic, mass-dependent isotopic variations within and between natural materials such as marine sediments and pore waters, sea water, ferromanganese crusts and nodules, igneous rocks and molybdenites (e.g., Anbar et al., 2001; Barling et al., 2001; Siebert et al., 2001, 2003, 2005; McManus et al., 2002; Nägler et al., 2005). Several analytical techniques have been used for Mo isotopic analyses by MC-ICP-MS, including different methods for the separation of Mo from the sample matrix and the correction for instrumental mass bias. Some studies of Mo (e.g., Anbar et al., 2001; Barling et al., 2001) used SSB with zirconium as an external monitor of instrumental mass bias to obtain a precision of ± 0.13‰/AMU (2σ) on samples and ± 0.05‰/AMU (2σ) on pure solution standards[1]. The difference in precision is thought to result from a matrix effect for natural samples (Barling et al., 2001). Other studies of Mo (e.g., Siebert et al., 2001, 2003) used double spiking to improve the precision to ± 0.02–0.03‰/AMU (2σ) for both samples and standards. Although the double-spike correction for instrumental mass bias is thought to largely avoid both matrix effects and the effects of isotopic fractionation during the separation of molybdenum from a sample (Siebert et al., 2001), this technique is more complex than SSB and may be more susceptible to memory effects (e.g., Albarède et al., 2004).

[1] Mass-dependent variations in the isotopic composition of Mo are reported using different isotope ratios by different laboratories (e.g., $^{97}Mo/^{95}Mo$ or $^{98}Mo/^{95}Mo$). Since the relative precision (in per mil) of different Mo isotope ratios using a given analytical technique is observed to depend mostly on the mass difference between the isotopes under consideration, we present estimates of precision on a "per AMU" basis to facilitate comparison between laboratories. For example, Barling et al. (2001) report a $\pm 2\sigma$ precision of ± 0.25‰ for measurements of mass-dependent variations in the $^{97}Mo/^{95}Mo$ ratio of natural samples, which corresponds to ± 0.13‰/AMU.

Here we present a detailed study of the ability of MC-ICP-MS to determine, both precisely and accurately, the natural mass-dependent isotopic variations of Mo extracted from molybdenite using SSB. In particular, we focus on a detailed evaluation of potential matrix effects in the MC-ICP-MS. Our methods for the chemical separation and mass spectrometric analysis of Mo are modified from the procedures developed by Anbar et al. (2001) and Barling et al. (2001). The main objective of this study is to determine if the SSB method of correcting for the effects of instrumental mass bias can produce data with a precision that is similar to the double-spike data of Siebert et al. (2001). In addition, five molybdenites of hydrothermal origin, representing a range of molybdenite-forming environments, were analyzed for their Mo isotopic compositions.

2. Preparation of Mo and Zr solution standards and a ^{97}Mo tracer solution

Several different solution standards and a ^{97}Mo-enriched isotopic tracer solution were used for this study. Two high-purity shelf solution standards were used. A 1000 mg/l Mo solution standard was purchased from Spex Certiprep, Inc. (catalog # CLMO9-2Y and lot # CL2-43MO) and a 1000 μg/ml Zr solution standard (stock # 13875 and lot # 201746B) was purchased from Alfa Aesar, a Johnson Matthey Co. Each of these solutions was diluted to a concentration of 15 μg/g in 0.5M HNO_3 and stored in Teflon FEP bottles for further dilution as needed. In this report, these shelf solution standards are referred to as the "Mo solution standard" and "Zr solution standard." In addition, an in-house gravimetric Mo solution standard was prepared from a 99.97% pure Mo wire purchased from Aldrich Chemical Co. (product # 26,690-6 and lot # 11418AU). This concentrated solution and a gravimetric dilution of it were stored in Teflon FEP bottles. This standard is referred to as the "Mo wire standard." A Mo isotopic tracer solution was prepared from a ^{97}Mo-enriched high-purity Mo metal purchased from the Oak Ridge National Laboratory (batch # 159791). This concentrated tracer solution and a gravimetric dilution of it were also stored in Teflon FEP bottles. The isotopic composition of the dilute ^{97}Mo tracer was determined by MC-ICP-MS to be 94.2% pure ^{97}Mo. The concentration of the dilute ^{97}Mo tracer was calibrated by MC-ICP-MS against the dilute Mo wire standard to a precision of 0.02% ($\pm 2\sigma_m$; $n=5$). Finally, a ^{97}Mo-enriched isotopic standard, termed UMD-A, was prepared by mixing the concentrated Mo wire standard with the dilute ^{97}Mo isotopic tracer to give an expected 1.00‰ increase in the ^{97}Mo/^{95}Mo ratio of the original Mo wire standard.

3. Mo separation and purification

A low-blank, high yield two-column chemistry procedure was used to maximize the removal of matrix elements from the samples and minimize the chromatographic isotopic fractionation of Mo. High-purity reagents were used for all analyses in this study. Mineral acids (HF, HCl and HNO_3) were purified by subboiling distillation. Water was purified by passing distilled water through an 18 MΩ de-ionization system. Molybdenite samples (Table 1) and a black shale reference material, MQSB-1 [prepared from the Mecca Quarry Shale described by Coveney and Glascock (1989) and Glascock et al. (1996)], were digested in a 1:1 mixture of concentrated HF:HNO_3 to attack silicate minerals. After drying completely, the samples were re-digested in a 40:60 mixture of concentrated HNO_3:HCl, which effectively dissolves molybdenite, and dried. At this stage, the molybdenites were a dark blue color, except for samples HV-1, HV-2 and Mt. T, which contained pale yellow impurities (consistent with

Table 1
Descriptions of the molybdenite samples used for this study

SN
Molybdenite from a quartz-molybdenite vein sample from Molybdenite Creek, Sierra Nevada Batholith, north of Yosemite National Park. The two molybdenite samples analyzed in this study, SN-1 and SN-2, were picked from different spots on fresh surfaces of the vein. Both were coarse-grained, flaky, and free of other minerals.

855111
Molybdenite sample from the Ichiman W–Mo deposit, Komaki mine, Shimane Prefecture, SW Japan. The analyzed sample was coarse-grained, flaky, and free of other minerals.

Mt. T
Molybdenite from the porphyry Mo–Cu deposit from Mount Tolman (NE Washington). The analyzed sample was fine-grained, massive, and contained large amounts of inter-grown minerals such as quartz and feldspar.

HV
Molybdenite from the Highland Valley porphyry Cu–Mo deposit of British Columbia, which is associated with the Guichon Creek Batholith. The analyzed sample was fine-grained, massive, and contained small amounts of inter-grown minerals such as quartz and feldspar.

UR-2
Molybdenite from the Urad Climax-type porphyry Mo deposit, Colorado Mineral Belt, Colorado. The analyzed sample was fine-grained, flaky, and free of other minerals.

Table 2
Mo isotopic data for solution standards and molybdenites relative to the Mo solution standard

	Simple standard-sample bracketing						External normalization standard-sample bracketing					
	$\delta^{97/95}$Mo	$\delta^{98/95}$Mo	$\delta^{100/95}$Mo	$\delta^{97/95}$Mo	$\delta^{98/95}$Mo	$\delta^{100/95}$Mo	$\delta^{97/95}$Mo	$\delta^{98/95}$Mo	$\delta^{100/95}$Mo	$\delta^{97/95}$Mo	$\delta^{98/95}$Mo	$\delta^{100/95}$Mo
	‰			‰/AMU			‰			‰/AMU		
Mo solution standard												
Mo+Zr	−0.010	−0.014	−0.025	−0.005	−0.005	−0.005	0.04	0.04	0.08	0.02	0.01	0.02
$\pm 2\sigma$	0.059	0.067	0.095	0.029	0.022	0.019	0.24	0.36	0.58	0.12	0.12	0.12
$\pm 2\sigma_m$ ($n=6$)	0.024	0.027	0.039	0.012	0.009	0.008	0.10	0.15	0.24	0.05	0.05	0.05
Mo only	0.014	0.009	0.011	0.007	0.003	0.002						
$\pm 2\sigma$	0.045	0.052	0.087	0.022	0.017	0.017						
$\pm 2\sigma_m$ ($n=8$)	0.016	0.018	0.031	0.008	0.006	0.006						
Average	0.004	−0.001	−0.005	0.002	0.000	−0.001						
$\pm 2\sigma$	0.054	0.061	0.094	0.027	0.020	0.019						
$\pm 2\sigma_m$ ($n=14$)	0.015	0.016	0.025	0.007	0.005	0.005						
Mo wire standard												
Mo+Zr	0.085	0.120	0.199	0.042	0.040	0.040	0.15	0.23	0.37	0.07	0.08	0.07
$\pm 2\sigma$	0.067	0.099	0.179	0.034	0.033	0.036	0.23	0.35	0.55	0.11	0.12	0.11
$\pm 2\sigma_m$ ($n=11$)	0.020	0.030	0.054	0.010	0.010	0.011	0.07	0.10	0.17	0.03	0.03	0.03
Mo only	0.090	0.130	0.214	0.045	0.043	0.043						
$\pm 2\sigma$	0.064	0.092	0.144	0.032	0.031	0.029						
$\pm 2\sigma_m$ ($n=15$)	0.016	0.024	0.037	0.008	0.008	0.007						
Average	0.088	0.126	0.207	0.044	0.042	0.041						
$\pm 2\sigma$	0.064	0.093	0.157	0.032	0.031	0.031						
$\pm 2\sigma_m$ ($n=26$)	0.013	0.018	0.031	0.006	0.006	0.006						
UMD-A Mo isotopic solution standard												
Mo+Zr	1.086	0.138	0.209	0.543	0.046	0.042	1.14	0.21	0.34	0.57	0.07	0.07
$\pm 2\sigma$	0.061	0.085	0.138	0.031	0.028	0.028	0.29	0.45	0.72	0.14	0.15	0.14
$\pm 2\sigma_m$ ($n=10$)	0.019	0.027	0.044	0.010	0.009	0.009	0.09	0.14	0.23	0.05	0.05	0.05
Mo only	1.076	0.122	0.183	0.538	0.041	0.037						
$\pm 2\sigma$	0.045	0.068	0.107	0.023	0.023	0.021						
$\pm 2\sigma_m$ ($n=15$)	0.012	0.018	0.028	0.006	0.006	0.006						
Average	1.080	0.129	0.193	0.540	0.043	0.039						
$\pm 2\sigma$	0.052	0.075	0.120	0.026	0.025	0.024						
$\pm 2\sigma_m$ ($n=25$)	0.010	0.015	0.024	0.005	0.005	0.005						
SN-1 molybdenite (98.6% yield)												
Mo+Zr	0.218	0.322	0.521	0.109	0.107	0.104	0.24	0.34	0.56	0.12	0.11	0.11
$\pm 2\sigma$	0.137	0.214	0.405	0.069	0.071	0.081	0.12	0.19	0.35	0.06	0.06	0.07
$\pm 2\sigma_m$ ($n=6$)	0.056	0.087	0.166	0.028	0.029	0.033	0.05	0.08	0.14	0.02	0.03	0.03
Mo only	0.238	0.355	0.573	0.119	0.118	0.115						
$\pm 2\sigma$	0.032	0.019	0.030	0.016	0.006	0.006						
$\pm 2\sigma_m$ ($n=3$)	0.019	0.011	0.017	0.009	0.004	0.003						
Average	0.224	0.333	0.539	0.112	0.111	0.108						
$\pm 2\sigma$	0.111	0.172	0.325	0.056	0.057	0.065						
$\pm 2\sigma_m$ ($n=9$)	0.037	0.057	0.108	0.019	0.019	0.022						
SN-2 molybdenite (97.7% yield)												
Mo+Zr	0.296	0.439	0.728	0.148	0.146	0.146	0.20	0.31	0.50	0.10	0.10	0.10
$\pm 2\sigma$	0.054	0.041	0.078	0.027	0.014	0.016	0.26	0.35	0.56	0.13	0.12	0.11
$\pm 2\sigma_m$ ($n=4$)	0.027	0.021	0.039	0.014	0.007	0.008	0.13	0.17	0.28	0.06	0.06	0.06
Mo only	0.275	0.423	0.686	0.138	0.141	0.137						
$\pm 2\sigma$	0.034	0.053	0.100	0.017	0.018	0.020						
$\pm 2\sigma_m$ ($n=6$)	0.014	0.022	0.041	0.007	0.007	0.008						
Average	0.284	0.429	0.703	0.142	0.143	0.141						
$\pm 2\sigma$	0.046	0.049	0.097	0.023	0.016	0.019						
$\pm 2\sigma_m$ ($n=10$)	0.014	0.015	0.031	0.007	0.005	0.006						

Table 2 (*continued*)

	Simple standard-sample bracketing						External normalization standard-sample bracketing					
	$\delta^{97/95}$Mo	$\delta^{98/95}$Mo	$\delta^{100/95}$Mo	$\delta^{97/95}$Mo	$\delta^{98/95}$Mo	$\delta^{100/95}$Mo	$\delta^{97/95}$Mo	$\delta^{98/95}$Mo	$\delta^{100/95}$Mo	$\delta^{97/95}$Mo	$\delta^{98/95}$Mo	$\delta^{100/95}$Mo
	‰			‰/AMU			‰			‰/AMU		
855111 molybdenite (99.5% yield)												
Mo+Zr	0.771	1.157	1.889	0.386	0.386	0.378	0.77	1.14	1.87	0.39	0.38	0.37
$\pm 2\sigma$	0.047	0.099	0.174	0.023	0.033	0.035	0.53	0.84	1.39	0.27	0.28	0.28
$\pm 2\sigma_m$ ($n=3$)	0.027	0.057	0.100	0.014	0.019	0.020	0.31	0.48	0.80	0.15	0.16	0.16
Mo only	0.751	1.117	1.835	0.376	0.372	0.367						
$\pm 2\sigma$	0.042	0.053	0.085	0.021	0.018	0.017						
$\pm 2\sigma_m$ ($n=4$)	0.021	0.027	0.042	0.010	0.009	0.008						
Average	0.760	1.134	1.859	0.380	0.378	0.372						
$\pm 2\sigma$	0.045	0.080	0.130	0.023	0.027	0.026						
$\pm 2\sigma_m$ ($n=7$)	0.017	0.030	0.049	0.009	0.010	0.010						
Mt. T molybdenite (98.3% yield)												
Mo+Zr	0.174	0.258	0.412	0.087	0.086	0.082	0.09	0.12	0.18	0.04	0.04	0.04
$\pm 2\sigma$	0.106	0.176	0.318	0.053	0.059	0.064	0.20	0.29	0.51	0.10	0.10	0.10
$\pm 2\sigma_m$ ($n=5$)	0.048	0.079	0.142	0.024	0.026	0.028	0.09	0.13	0.23	0.04	0.04	0.05
Mo only	0.143	0.202	0.332	0.072	0.067	0.066						
$\pm 2\sigma$	0.006	0.016	0.016	0.003	0.005	0.003						
$\pm 2\sigma_m$ ($n=3$)	0.004	0.009	0.009	0.002	0.003	0.002						
Average	0.162	0.237	0.382	0.081	0.079	0.076						
$\pm 2\sigma$	0.087	0.145	0.254	0.043	0.048	0.051						
$\pm 2\sigma_m$ ($n=8$)	0.031	0.051	0.090	0.015	0.017	0.018						
HV-1 molybdenite (99.0% yield)												
Mo+Zr	−0.529	−0.772	−1.252	−0.264	−0.257	−0.250	−0.62	−0.93	−1.55	−0.31	−0.31	−0.31
$\pm 2\sigma$	0.039	0.061	0.114	0.020	0.020	0.023	0.27	0.41	0.68	0.13	0.14	0.14
$\pm 2\sigma_m$ ($n=3$)	0.023	0.035	0.066	0.011	0.012	0.013	0.16	0.24	0.39	0.08	0.08	0.08
Mo only	−0.526	−0.786	−1.282	−0.263	−0.262	−0.256						
$\pm 2\sigma$	0.045	0.070	0.130	0.022	0.023	0.026						
$\pm 2\sigma_m$ ($n=4$)	0.022	0.035	0.065	0.011	0.012	0.013						
Average	−0.527	−0.780	−1.269	−0.263	−0.260	−0.254						
$\pm 2\sigma$	0.039	0.063	0.117	0.020	0.021	0.023						
$\pm 2\sigma_m$ ($n=7$)	0.015	0.024	0.044	0.007	0.008	0.009						
HV-2 molybdenite (97.7% yield)												
Mo+Zr	−0.501	−0.741	−1.217	−0.250	−0.247	−0.243	−0.48	−0.70	−1.13	−0.24	−0.23	−0.23
$\pm 2\sigma$	0.031	0.039	0.048	0.016	0.013	0.010	0.63	0.93	1.50	0.32	0.31	0.30
$\pm 2\sigma_m$ ($n=3$)	0.018	0.022	0.028	0.009	0.007	0.006	0.36	0.54	0.86	0.18	0.18	0.17
Mo only	−0.490	−0.730	−1.182	−0.245	−0.243	−0.236						
$\pm 2\sigma$	0.026	0.034	0.060	0.013	0.011	0.012						
$\pm 2\sigma_m$ ($n=3$)	0.015	0.020	0.035	0.008	0.007	0.007						
Average	−0.495	−0.736	−1.199	−0.248	−0.245	−0.240						
$\pm 2\sigma$	0.028	0.035	0.062	0.014	0.012	0.012						
$\pm 2\sigma_m$ ($n=6$)	0.012	0.014	0.025	0.006	0.005	0.005						
UR-2 molybdenite (99.0% yield)												
Mo+Zr	0.407	0.603	0.982	0.204	0.201	0.196	0.34	0.49	0.82	0.17	0.16	0.16
$\pm 2\sigma$	0.097	0.144	0.240	0.048	0.048	0.048	0.18	0.25	0.41	0.09	0.08	0.08
$\pm 2\sigma_m$($n=6$)	0.040	0.059	0.098	0.020	0.020	0.020	0.07	0.10	0.17	0.04	0.03	0.03
Mo only	0.393	0.594	0.969	0.196	0.198	0.194						
$\pm 2\sigma$	0.003	0.010	0.054	0.001	0.003	0.011						
$\pm 2\sigma_m$ ($n=3$)	0.002	0.006	0.031	0.001	0.002	0.006						
Average	0.402	0.600	0.977	0.201	0.200	0.195						
$\pm 2\sigma$	0.078	0.115	0.192	0.039	0.038	0.038						
$\pm 2\sigma_m$ ($n=9$)	0.026	0.038	0.064	0.013	0.013	0.013						

All data were collected at SDSU. The signal intensities of Mo and Zr between the sample and the bracketing standard were matched within 5% for each analysis. The ^{95}Mo/^{90}Zr ratio of each Mo+Zr measurement was ≥5.4. Data in a single row are averages of the same group of analyses, but were corrected for mass bias using different methods.

the presence of other minerals in these samples; Table 1). In this study, MQSB-1 was used solely for the purpose of column calibration. Completely separate dissolutions of the molybdenites were used for the purpose of the final Mo isotopic analyses (Table 2) and experiments described below.

Since molybdenites (MoS_2) are assumed to be essentially pure Mo (in terms of cations), previous studies of molybdenites simply dissolved and diluted the mineral for mass spectrometry without separating the Mo from the sample matrix (e.g., Anbar et al., 2001; Barling et al., 2001). We tested this assumption using three molybdenites (UR-2, HV and 855111). These samples were dissolved, diluted and analyzed qualitatively on the Element 2 single-collector high-resolution ICP-MS at the University of Maryland (UMD) to determine which, if any, other elements were present at significant levels in the samples. A total of 50 elements were checked in low-resolution mode by scanning the following masses a total of 10 times for each solution: ^{23}Na, ^{24}Mg, ^{27}Al, ^{43}Ca, ^{45}Sc, ^{47}Ti, ^{51}V, ^{52}Cr, ^{55}Mn, ^{57}Fe, ^{59}Co, ^{60}Ni, ^{63}Cu, ^{66}Zn, ^{69}Ga, ^{72}Ge, ^{82}Se, ^{85}Rb, ^{88}Sr, ^{89}Y, ^{90}Zr, ^{93}Nb, ^{95}Mo, ^{101}Ru, ^{103}Rh, ^{105}Pd, ^{107}Ag, ^{111}Cd, ^{115}In, ^{118}Sn, ^{121}Sb, ^{133}Cs, ^{137}Ba, ^{140}Ce, ^{146}Nd, ^{147}Sm, ^{157}Gd, ^{172}Yb, ^{175}Lu, ^{178}Hf, ^{181}Ta, ^{182}W, ^{185}Re, ^{189}Os, ^{193}Ir, ^{205}Tl, ^{208}Pb, ^{209}Bi, ^{232}Th and ^{238}U. Prior to the introduction of each sample into the Element 2 using a Glass Expansion MicroMist borosilicate glass nebulizer with an uptake rate of ~400 μl/min and a 20-ml Glass Expansion Cinnabar Cyclonic spray chamber, on-peak zeros were measured while aspirating the 0.5 M HNO_3 that was used to dilute the samples. For each mass, the on-peak zero signal intensities were subtracted from the signal intensities of the subsequent sample solution. An element was assumed to be present in the sample solution only if its signal intensity (after on-peak zero subtraction) was greater than the combined $\pm 2\sigma_m$ uncertainties on the average signal intensities of both the on-peak zero and sample measurements. The final signal intensities for each mass were normalized to the signal intensity of ^{95}Mo, and atomic ratios were calculated. For each of the molybdenites, Ca was found to be the dominant element in the samples besides Mo (making up ~90–97% of the elements other than Mo on an atomic basis), corresponding to atomic Ca/Mo ratios of ~0.60, 0.65 and 0.36 for UR-2, HV and 855111, respectively (Fig. 1a). Other elements found at levels greater than 1% of the molybdenum abundance (i.e., X/Mo ratios > 0.01) in a particular sample were Al, Ni and Cu. Elements found at levels greater than 0.1% of the molybdenum abundance (i.e., X/Mo ratios > 0.001) in a particular sample were Mg, Cr, Mn, Cu, Sr, Cd, W, Re and Pb. Given the relatively high Ca contents of these samples, and Ni and Cu to a lesser extent, it was necessary to separate the Mo from each molybdenite to ensure that matrix effects do not significantly bias the isotopic data.

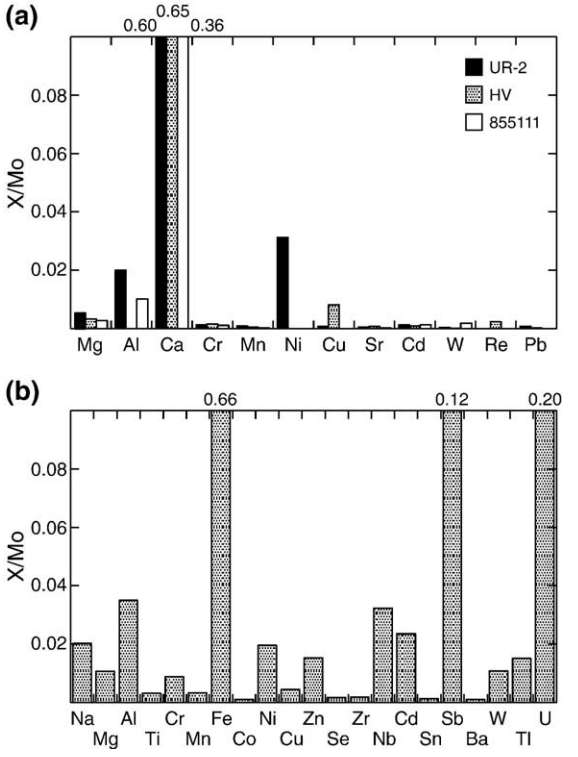

Fig. 1. Graphical representation of the matrix elements observed in (a) molybdenites prior to the chemical separation of their Mo and (b) the MQSB-1 standard after it was passed through the anion exchange resin column to separate its Mo. The ratio, X/Mo, represents the atomic proportion of a given element, X, relative to Mo.

The details of our procedure are presented in Table 3. Briefly, two columns were used to separate the Mo from each sample. The first column used ~10 ml of precleaned AG1-X8 (100–200 mesh) anion exchange resin to remove Zr and most other matrix elements. An extensive resin pre-cleaning procedure was required to obtain a sufficiently low Mo blank (~0.8 ng) for this procedure (Table 3). The digested sample was dissolved in 6 M HCl, dried completely and re-dissolved in 6 M HCl. At this stage, all samples were split into a large and small aliquot to determine the total recovery of Mo. The small aliquot was spiked with the gravimetrically calibrated, ^{97}Mo-enriched isotopic tracer to determine the amount of Mo in the solution. Prior to loading the sample, the column was further cleaned with 0.01 M HCl and 1 M HCl and conditioned in 6 M HCl. The sample was loaded in 6 M HCl and the resin was washed with 6 M HCl. This step effectively removes

Table 3
Summary of Mo separation chemistry

	Reagent	# of c.v.
Resin pre-cleaning		
Resin	AG1-X8 (100–200 mesh)	
Clean	8 M HNO_3	2
Clean	18 MΩ H_2O	2
Clean	6 M HCl	2
Clean	18 MΩ H_2O	2
Clean	1 M HCl	2
Clean	18 MΩ H_2O	2
Column #1		
Resin	AG1-X8 (100–200 mesh)	
Clean	0.01 M HCl	10
Clean	1 M HCl	5
Condition	6 M HCl	3
Load	6 M HCl	<0.5
Wash	6 M HCl	4
Wash	0.1 M HF+0.01 M HCl	4
Collect Mo	1 M HCl	12
Collect Mo	5 M HNO_3	5
Column #2		
Resin	AG50W-X8 (200–400 mesh)	
Condition	1.4 M HCl	5.7
Load (Collect Mo)	1.4 M HCl	<0.5
Collect Mo	1.4 M HCl	2.3
Clean	6 M HCl	57

The resin-bed dimensions were 0.6 cm wide and 34 cm long for column #1 and 0.6 cm wide and 12.5 cm long for column #2. The anion exchange resin from column #1 was discarded after each use. The cation exchange resin from column #2 was cleaned and re-used after each sample. c.v. = column volume.

Zr and most other matrix elements from the sample, with the notable exception of Fe. Unlike previous studies using AG1-X8 in 6 M HCl (e.g., Barling et al., 2001), we next washed the resin with a mixture of 0.1 M HF+0.01 M HCl to remove most of the Fe prior to Mo elution. Finally, the Mo was collected in 1 M HCl followed by 5 M HNO_3. Elution of the Mo with two different acids helped to improve recovery. Next, the sample was dried completely, dissolved in 6 M HCl and dried. A second column used ~3.5 ml of AG50W-X8 (200–400 mesh) cation exchange resin to remove any remaining Fe, and several other elements (e.g., U, Al, Ni, Mg and Zn), from the sample. Mo blanks for the cation exchange resin column ranged from ~1 to 3 ng. The sample was dissolved in 1.4 M HCl and loaded onto the pre-conditioned resin. The Mo was collected in this elutant and an additional 1.4 M HCl wash. A small aliquot of this solution was spiked with the ^{97}Mo tracer to determine the net recovery of Mo. The total yield of Mo from this two-column procedure ranged from 97.7% to 99.5% for the molybdenites (Table 2). After the recovery of Mo was determined, the sample was dried, dissolved in 0.5 M HNO_3 and stored in a Teflon PFA beaker. Immediately prior to analysis, each sample solution was refluxed for 1 h at 100 °C and cooled to room temperature. Aliquots of all samples and standards used in this study were prepared on the day of analysis. Finally, it is important to note that all isotope-dilution measurements were performed on the Nu Plasma using an internal mass-bias correction and separate reagents, chromatographic columns and beakers to eliminate any possibility of cross-contamination between the ^{97}Mo-enriched tracer and the samples.

The efficiency of the Mo separation was evaluated using MQSB-1 and selected molybdenites. First, MQSB-1 was passed through the anion exchange resin column and the solution was analyzed qualitatively using the Element 2 for other elements relative to Mo as described previously (Fig. 1b). In this case, the Mo was collected only in 1 M HCl because the experiment was completed before it was discovered that the additional 5 M HNO_3 improved the recovery of Mo. The most abundant element found in the solution besides Mo was Fe (making up ~55% of the elements other than Mo on an atomic basis) with a Fe/Mo ratio of ~0.66. The next most abundant elements found at greater than 1% of the Mo abundance were U (17%; U/Mo=0.20), Sb (9.7%; Sb/Mo=0.12), Al (2.9%; Al/Mo=0.03), Nb (2.7%; Nb/Mo=0.03), Cd (2.0%; Cd/Mo=0.02), Na (1.7%; Na/Mo=0.02), Ni (1.6%; Ni/Mo=0.02), Zn (1.3%; Zn/Mo=0.02), Tl (1.3%; Tl/Mo=0.02), W (0.9%; W/Mo=0.01) and Mg (0.9%; Mg/Mo=0.01). Other elements found above 0.1% of the Mo abundance were Ti, Cr, Mn, Co, Cu, Se, Zr, Sn and Ba. This test showed that a second chromatographic column is necessary, despite the nearly quantitative elution of Fe on the first column, to remove the remaining Fe and as many of these other elements as possible. Second, the MQSB-1 Mo cut solution from the anion column was passed through the cation column. In addition, the molybdenites that were examined before chemistry (UR-2, HV and 855111) were passed through both the anion and cation columns. Again, these experiments were done by collecting Mo only in 1 M HCl from the anion column. The solutions were analyzed on the Element 2 to determine the nature and amount of other elements that pass into the Mo cut. The MQSB-1 Mo cut contained small amounts of Nb (Nb/Mo=0.003), Cd (Cd/Mo=0.0008), Sb (Sb/Mo=0.007), W (W/Mo=0.0008) and Tl (Tl/Mo=0.0006). Elements present in the molybdenite solutions were Mg (Mg/Mo=0.01), Cu (Cu/Mo=0.01), Cd (Cd/Mo=0.0009) and Ba (Ba/Mo=0.002–0.003). This experiment confirms that the two-pass column chemistry effectively removes most

elements from the sample. However, it is possible that the elution of the remaining Mo from the anion exchange resin in 5 M HNO_3 may cause additional elements (e.g., Nb) to pass into the Mo cut. Further study is required to examine this possibility, but it is important to note that this will not affect our Mo isotopic data for the molybdenites because these samples are thought to be essentially free of Nb (and samples UR-2, HV and 855111 are known to lack Nb).

4. Mass spectrometry

The Mo isotope ratios were measured on a Nu Plasma MC-ICP-MS at either UMD or the San Diego State University (SDSU). Sample solutions (in 0.5 M HNO_3) were introduced into the system in different ways. At UMD, samples were introduced using a Cetac Aridus desolvating system and PFA nebulizer with an uptake rate of ~30 μl/min. At SDSU, samples were introduced using a Nu Instruments DSN-100 desolvating system and Glass Expansion MicroMist borosilicate glass nebulizer with an uptake rate of ~100 μl/min. All samples and standards were run for 30 ratios in 2 blocks of 15 ratios each (see Table 4 for the mass array used in this study). Zeros were measured for 20 s once per block using the electrostatic analyzer located before the magnet to completely deflect the ion beam (the magnet setting was 0.5 AMU lower than the masses listed for sequence 1 on Table 4). After each analysis, the sample was washed from the system over six min using three sequential solutions of 0.5 M HNO_3. The residual signal was typically $<6\times10^{-14}$ A of total Mo, which is insignificant. An autosampler was used to maintain constant timing for each analysis (15 min total). The typical signal intensities were 2.6×10^{-10} A of total Mo ($1.4–3.7\times10^{-10}$ A range). The total amount of Mo consumed per analysis was typically ~0.7 μg, which corresponds to a Mo concentration of ~0.8 μg/g for sample and standard solutions.

Two different variants of SSB were employed to correct the measured Mo isotope ratios for the effects of instrumental mass bias: an external normalization using Zr added to the sample as a monitor of instrumental mass bias ("Zr doping") and/or a simple SSB correction based solely on the measured Mo isotope ratios (whether Zr was present in the solution or not). In both cases, each sample was run between two bracketing Mo solution standards to monitor the magnitude and temporal drift of the instrumental mass bias. In the first case (external normalization SSB), instrumental mass bias was corrected using a two-step procedure (e.g., Carlson et al., 2001). The measured $^{91}Zr/^{90}Zr$ ratio was used to calculate the fractionation factor for Zr, β_{Zr}, assuming the exponential law of Russell et al. (1978):

$$R^{Zr}_{Meas.} = R^{Zr}_{Frac.Corr.} \times \left(\frac{M_{91_{Zr}}}{M_{90_{Zr}}}\right)^{\beta_{Zr}}$$

where $R^{Zr}=^{91}Zr/^{90}Zr$ and M is the mass of the isotope (in AMU). The "*Meas.*" and "*Frac. Corr.*" subscripts refer to the measured and fractionation-corrected (or "true") isotope ratios, respectively. In this study, $R^{Zr}_{Frac.Corr.}=0.21814$. The Zr fractionation factor was then used to correct the measured Mo isotope ratios (using a similar equation written for Mo), assuming that (1) the two elements fractionate according to the exponential law and (2) $\beta_{Mo}=\beta_{Zr}$. Following this initial correction, the Mo isotope ratios were then corrected a second time using the bracketing standards (themselves corrected using Zr) by linear interpolation. In the second case (simple SSB), the measured Mo isotope ratios of the unknowns were corrected using a linear interpolation of the measured Mo isotope ratios of the bracketing standards. All analyses that were doped with Zr were also corrected using simple SSB (i.e., the Zr was ignored). These correction schemes are examined in the following discussion. Finally, it is important to note that we also evaluated the empirical method of correcting for the effects of instrumental mass bias developed by Maréchal et al. (1999). However, the drift in the instrumental mass bias on the Nu Plasma at both UMD and SDSU was typically too small to use this approach successfully.

For each analysis, the Mo isotopes that are free of Zr interferences (95, 97, 98 and 100) were measured on Faraday collectors in the first of two static sequences (Table 4). In addition, ^{99}Ru was measured in this sequence to correct for the presence of ^{100}Ru (a potential isobaric interference with ^{100}Mo), although

Table 4
Collector positions for Mo isotopic measurements by MC-ICP-MS

Sequence	Integration time (s)	High 6	High 5	High 4	High 2	Low 2	Low 4	Low 5
(1)	5	^{100}Mo	^{99}Ru	^{98}Mo	^{97}Mo	^{95}Mo		
(2)	5						^{91}Zr	^{90}Zr

Table 5
Mo isotopic data for the UMD-A Mo isotopic solution standard relative to the Mo wire standard

	Simple standard-sample bracketing						External normalization standard-sample bracketing					
	$\delta^{97/95}$Mo	$\delta^{98/95}$Mo	$\delta^{100/95}$Mo	$\delta^{97/95}$Mo	$\delta^{98/95}$Mo	$\delta^{100/95}$Mo	$\delta^{97/95}$Mo	$\delta^{98/95}$Mo	$\delta^{100/95}$Mo	$\delta^{97/95}$Mo	$\delta^{98/95}$Mo	$\delta^{100/95}$Mo
	‰			‰/AMU			‰			‰/AMU		
Observed												
Mo+Zr	1.00	0.02	0.01	0.501	0.006	0.002	0.99	−0.02	−0.04	0.494	−0.006	−0.007
Mo only	0.99	−0.01	−0.03	0.493	−0.003	−0.006						
Average	0.99	0.00	−0.01	0.496	0.001	−0.003						
Predicted	1.00	0.01	0.00	0.500	0.004	0.000	1.00	0.01	0.00	0.500	0.004	0.000

All data were collected at SDSU and are recalculated from the same analyses of these standards reported in Table 2.

the ^{99}Ru was typically below detection. The second static sequence was used to measure the ^{91}Zr/^{90}Zr ratio for samples that were corrected for instrumental mass bias using external normalization SSB. The other Mo isotopes (92, 94 and 96) were also measured in the first sequence, but these data are not reported due to the inaccuracy of correcting for the large Zr interferences when this element is used to correct for instrumental mass bias. All final Mo isotopic data (Table 2) are reported using "delta" notation for Mo isotope 9X, which is defined as $\delta^{9X/95}\text{Mo} = 1000 \times \{[(^{9X}\text{Mo}/^{95}\text{Mo})_{\text{sample}}/(^{9X}\text{Mo}/^{95}\text{Mo})_{\text{standard}}] - 1\}$. Except for the data in Table 5, all $\delta^{9X/95}$Mo values in this study are expressed relative to the Mo solution standard, which was always used as the bracketing standard.

5. Evaluation of matrix effects

5.1. Automatrix effects

Automatrix effects may be present during SSB measurements by MC-ICP-MS, although these are typically noted to be a problem only for relatively high solute concentrations (e.g., Kehm et al., 2003). The extent of the automatrix effect on the measured Mo isotope ratios was evaluated (Fig. 2) by running the Mo solution standard (without Zr) alternately with another aliquot of this same solution. In one case (diamonds on Fig. 2), the same solution was analyzed repeatedly on one day. In two other cases (circles and squares on Fig. 2), the second solution was progressively diluted over the course of the day to determine the automatrix effect. Every other analysis was corrected for instrumental mass bias using simple SSB. These experiments show that when the concentration, and thus, signal intensity of the two solutions begin to diverge, the $\delta^{97/95}$Mo values begin to decrease significantly from the expected value of 0‰. In order to minimize this effect, the concentration of Mo in both samples and bracketing standards needs to be held constant within strict limits. In this study, the signal intensities of samples and standards were matched within 5%. This amounts to a maximum deviation of 0.005‰/AMU according to the equation of the best-fit line to the data in Fig. 2, which is negligible relative to the overall reproducibility of our measurements. However, additional work is required to determine if the presence of Zr in the analyte solution will enhance or mitigate the automatrix effect for Mo. Finally, it is important to note that this automatrix effect is characterized by a relative enhancement of the instrumental mass bias for the more concentrated solutions.

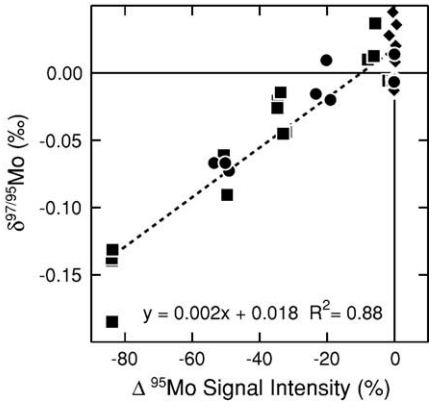

Fig. 2. Automatrix effects in the MC-ICP-MS. These data were collected over three separate analytical sessions (diamonds, circles and squares) on the Nu Plasma at SDSU by repeatedly analyzing the Mo solution standard (without Zr). In one case (diamonds), the same solution was analyzed repeatedly on one day. In two other cases (circles and squares), an aliquot of the Mo solution standard was progressively diluted over the course of the day (and run alternately with the original undiluted solution) to determine the nature and magnitude of the automatrix effect. The $\delta^{97/95}$Mo value (calculated using simple SSB) shows the ‰ deviation between the dilute solution compared to the concentrated solution (circles and squares) or every other analysis of a solution of constant Mo concentration (diamonds). The Δ^{95}Mo signal intensity represents the % difference in the signal intensity between the standard treated as an unknown and bracketing standards. Negative values indicate more dilute, low signal intensity solutions.

5.2. Matrix effects due to zirconium doping

The effect of varying the Mo/Zr ratio between the sample and bracketing standard solutions was determined using two different experiments during separate analytical sessions (circles and squares on Fig. 3). Both experiments used the Mo and Zr solution standards. In the first experiment (circles), the $^{95}Mo/^{90}Zr$ ratio was varied from 0.17 to 4.6 by changing the relative amounts of Mo and Zr in the solutions, without maintaining constant concentrations of either Mo or Zr. In this case, the solution with a $^{95}Mo/^{90}Zr=4.6$ was used as a bracketing standard. In the second experiment (squares), the $^{95}Mo/^{90}Zr$ ratio was varied from 0.60 to 10 by changing the relative amount of Zr in different aliquots of a single solution with a constant Mo concentration. In this case, the solution with a $^{95}Mo/^{90}Zr=5.3$ was used as a bracketing standard.

In the first experiment, both methods of correcting for instrumental mass bias display relatively large deviations of $\delta^{97/95}$Mo to negative values as the $^{95}Mo/^{90}Zr$ ratio decreases (up to ~1‰; Fig. 3). The exact origin of this matrix effect is unknown because too many factors were varied during the experiment. In the second experiment, the $\delta^{97/95}$Mo ratios of analyses that were corrected for instrumental mass bias using external normalization SSB display a shift to positive values (up to ~0.4‰) as the $^{95}Mo/^{90}Zr$ ratio of the solution decreases. Examination of the data shows that this effect results from a relative decrease in the instrumental mass bias for Zr as the concentration of Zr increases (and the $^{95}Mo/^{90}Zr$ ratio decreases), which is opposite to the automatrix effect previously observed for Mo. In contrast, the instrumental mass bias for Mo does not appear to be strongly affected by the large variations in the Zr concentration of the solution. Thus, the net effect is that the $\delta^{97/95}$Mo values become progressively under-corrected for instrumental mass bias as the $^{95}Mo/^{90}Zr$ ratio of the solution decreases. Furthermore, as expected from this interpretation, the $\delta^{97/95}$Mo values of analyses from the second experiment that were corrected for instrumental mass bias using simple SSB display little deviation as the $^{95}Mo/^{90}Zr$ ratio of the solution decreases. However, the slightly elevated $\delta^{97/95}$Mo values of analyses at the lowest $^{95}Mo/^{90}Zr$ ratios suggest that there may be a smaller matrix effect of unknown origin. Unlike some elements (e.g., Th and U using a VG P54 MC-ICP-MS; Pietruszka et al., 2002) it may not be possible to correct for these matrix effects in any simple fashion because the sense of the deviation of the Mo isotope ratios differed between the two sessions. However, for both of these experiments, the deviation of the $\delta^{97/95}$Mo values decreases as the $^{95}Mo/^{90}Zr$ ratios of the solutions increase. Thus, all of our samples and standards (Table 2) were analyzed at constant (within 5%) and high $^{95}Mo/^{90}Zr$ ratios (>5.4) to minimize these matrix effects. As previously noted, constant Mo/Zr ratios were maintained by matching the signal intensities, and thus, concentrations of both samples and bracketing standards (all parameters within 5%).

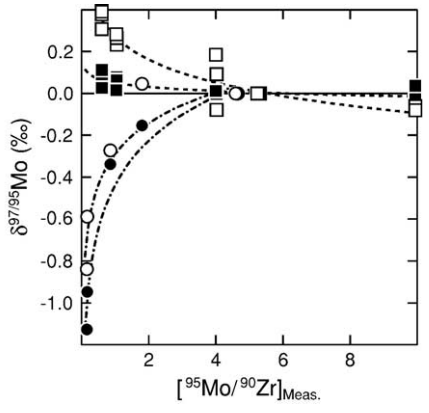

Fig. 3. Matrix effects in the MC-ICP-MS due to zirconium doping. These data were collected over two separate analytical sessions (circles and squares) on the Nu Plasma at UMD. The correction for instrumental mass bias was performed using both simple (closed symbols) and external normalization (open symbols) SSB.

5.3. Matrix effects due to other elements

The possibility of matrix effects from elements that were incompletely removed from the final Mo cuts by the two-pass column chemistry procedure was also evaluated: Nb, Cd, Sb, W and Tl (the elements present in the MQSB-1 cut) and, in addition, Na and Mg. For these experiments, the Mo and Zr solution standards were mixed together. Small amounts of highly concentrated high-purity element solutions were added to aliquots of this mixed Mo–Zr solution to give a range of matrix element concentrations that was higher than observed to be present in MQSB-1 after the two-pass column chemistry. In addition, each of the elements was added to one aliquot of the mixed Mo–Zr solution to create a multi-element matrix. This method of solution preparation ensured nearly constant Mo and Zr concentrations, and thus, Mo/Zr ratios, in both solutions. Before each measurement of a given matrix-element doped solution, the approximate atomic proportion of the matrix element compared to Mo was determined by scanning the relative intensities of one isotope of Mo and one isotope of the element at the following masses: ^{23}Na, ^{24}Mg, ^{93}Nb, ^{95}Mo, ^{111}Cd, ^{121}Sb, ^{182}W and ^{205}Tl.

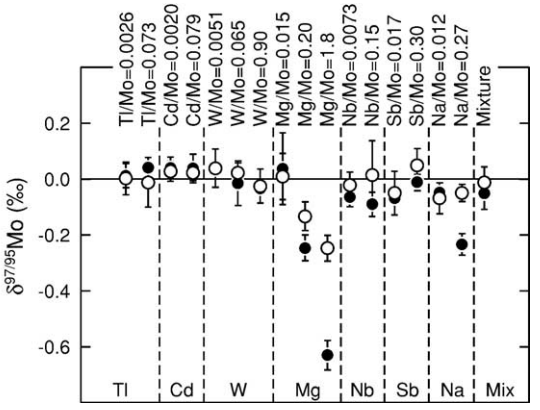

Fig. 4. Matrix effects in the MC-ICP-MS due to other elements. Each of these measurements was performed on the Nu Plasma at UMD. The correction for instrumental mass bias was performed using both simple (closed symbols) and external normalization (open symbols) SSB. Each point on the figure represents the average of 2–5 analyses. Error bars are the total range ($n=2$) or the $\pm 2\sigma_m$ values of the replicate measurements ($n \geq 3$). The atomic proportions of the mixture were Na/Mo=0.027, Mg/Mo=0.014, Nb/Mo=0.0090, Cd/Mo=0.045, Sb/Mo=0.018, W/Mo=0.0057 and Tl/Mo=0.0043.

The "zoom" lens of the Nu Plasma was re-tuned to produce a flat-topped peak for each element prior to measurement, but the other tuning parameters were left unchanged. Next, the matrix-element doped solution was run alternately with the original standard solution as a bracketing standard. In order to evaluate the effects of the matrix element on the Mo isotope ratios, instrumental mass bias was corrected using both methods (Fig. 4). These experiments show that matrix effects for these elements are generally small or absent within the precision of the measurements (at least for the matrix-element concentrations that were tested). The major exceptions are Mg and Na. In these two cases, external normalization SSB (open circles) works better than simple SSB (closed circles) to remove the matrix effect. An examination of the data indicates that the presence of the matrix element tends to decrease the relative instrumental mass bias of both Mo and Zr as the concentration of the matrix element increases. However, external normalization SSB still does not completely remove the matrix effect, which indicates that there is differential matrix effect on the Mo compared to the Zr. In all cases, it is important to note that the amount of element required to see a matrix effect is much greater than seen in our tests with molybdenites and MQSB-1 after they have been passed though the two-column chemistry procedure. Thus, we conclude that all three of the known matrix effects that might potentially affect the quality of our molybdenite analyses have been eliminated or controlled.

6. Results and discussion

6.1. Accuracy and precision

The accuracy and precision of our analytical techniques were evaluated using a range of approaches (see Fig. 5 for a summary). The simplest test of the precision is to examine the reproducibility of a single standard solution that has been analyzed repeatedly. This represents an ideal case because the sample is run rapidly without washing between analyses. We tested this with the Mo solution standard, using every other analysis as an unknown (Table 2). The expected results from this experiment are $\delta^{9X/95}$ values of 0‰ within the $\pm 2\sigma_m$ reproducibility (since the solution was run repeatedly). Our results show that, regardless of the method used for

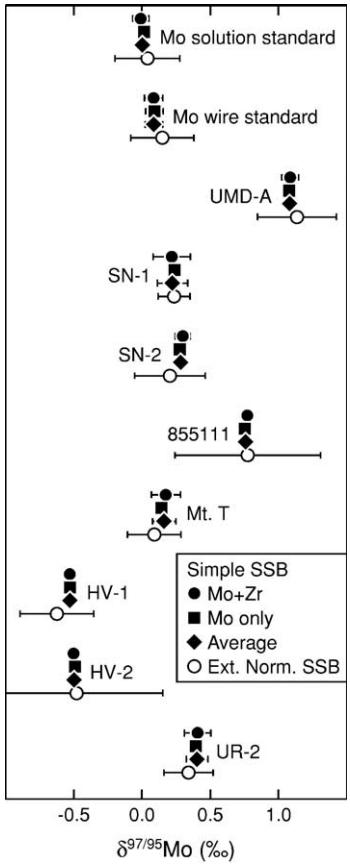

Fig. 5. Graphical comparison of the precision of our analytical techniques. Error bars are the $\pm 2\sigma$ values of the replicate measurements from Table 2 (not shown if smaller than the size of the symbols). The correction for instrumental mass bias was performed using both simple (closed symbols) and external normalization (open symbols) SSB. The closed circles, squares and diamonds represent (1) measurements when the Zr in the Zr-doped solution is ignored, (2) measurements without Zr and (3) the average of the two types of data, respectively.

the correction of instrumental mass bias, all ratios are within $\pm 2\sigma_m$ of 0‰. However, the precision resulting from each method differs significantly. The precision using external normalization SSB (0.12‰/AMU, $\pm 2\sigma$) is worse than either of the two experiments corrected using simple SSB (0.02‰/AMU, $\pm 2\sigma$, with or without Zr). Furthermore, it is important to note that there is no reduction in the precision of the measurements when the Zr in the Zr-doped solution is ignored. This means that it is acceptable to use Zr doping to monitor the presence of matrix effects from elements besides Mo or Zr, but use only the measured Mo isotope ratios and simple SSB. If different results are obtained using simple vs. external normalization SSB on Zr-doped samples, it may suggest the presence of a matrix effect (not observed in this study). However, the poorer precision that results from using external normalization SSB means that the matrix effects would have to be rather large before they are observed.

The precision of our data can also be evaluated using analyses of the Mo wire standard and the UMD-A Mo isotopic solution standard. This test of precision is more realistic because it includes the duration of sample washout, and thus, the potential for additional drift of the instrumental mass bias between analyses (memory effects from incomplete washout of Mo between analyses are negligible). The precision of these analyses is similar to the results for the Mo solution standard, depending on the method used for the instrumental mass-bias correction: ~0.11–0.15‰/AMU, $\pm 2\sigma$, using external normalization SSB and ~0.02–0.03‰/AMU, $\pm 2\sigma$, using simple SSB. Again, simple SSB is substantially more precise than external normalization SSB.

Interestingly, previous MC-ICP-MS studies of mass-dependent variations in the isotopic composition of Fe, Cu and Cd using both simple and external normalization SSB have noted the opposite behavior (e.g., Zhu et al., 2000b; Wombacher et al., 2003; Arnold et al., 2004). However, it is important to note that the inferior precision of simple SSB in these studies may have been influenced by two factors that favor external normalization SSB: (1) the natural samples used to evaluate the relative precision of simple vs. external normalization SSB in two of these studies (Wombacher et al., 2003; Arnold et al., 2004) are thought to have suffered from matrix effects due to the presence of elements besides the analyte (Cd or Fe) and/or (2) the samples and standards analyzed using external normalization SSB in two of these studies (Zhu et al., 2000b; Wombacher et al., 2003) contained a relatively large amount of the element (Zn or Ag) used for external normalization (e.g., Cu/Zn ~1 and Cd/Ag<2).

The large difference in precision between the two methods of correcting for instrumental mass bias observed in this study cannot be explained by a rapid fluctuation in the relative values of β_{Mo} and β_{Zr} between the time of measurement of the Mo isotope ratios in sequence 1 and the $^{91}Zr/^{90}Zr$ ratio in sequence 2. This possibility was tested (Table 6) using the $^{97}Mo/^{95}Mo$ and $^{98}Mo/^{95}Mo$ ratios from sequence 2 (with ^{98}Mo, ^{97}Mo and ^{95}Mo centered on the High 6, High 5 and High 2 Faraday collectors, respectively, when ^{91}Zr and ^{90}Zr are measured simultaneously as

Table 6
Mo isotopic data for solution standards relative to the Mo solution standard for sequence 2

	Simple standard-sample bracketing				External normalization standard-sample bracketing			
	$\delta^{97/95}$Mo	$\delta^{98/95}$Mo	$\delta^{97/95}$Mo	$\delta^{98/95}$Mo	$\delta^{97/95}$Mo	$\delta^{98/95}$Mo	$\delta^{97/95}$Mo	$\delta^{98/95}$Mo
	‰		‰/AMU		‰		‰/AMU	
Mo solution standard								
Mo+Zr	−0.001	−0.006	−0.001	−0.002	0.05	0.09	0.025	0.031
$\pm 2\sigma$	0.037	0.035	0.018	0.012	0.20	0.32	0.098	0.106
$\pm 2\sigma_m$ ($n=6$)	0.015	0.014	0.008	0.005	0.08	0.13	0.040	0.043
Mo wire standard								
Mo+Zr	0.081	0.124	0.041	0.041	0.16	0.24	0.078	0.081
$\pm 2\sigma$	0.067	0.112	0.034	0.037	0.22	0.31	0.110	0.102
$\pm 2\sigma_m$ ($n=11$)	0.020	0.034	0.010	0.011	0.07	0.09	0.033	0.031
UMD-A Mo isotopic solution standard								
Mo+Zr	1.089	0.139	0.545	0.046	1.14	0.22	0.569	0.073
$\pm 2\sigma$	0.048	0.072	0.024	0.024	0.29	0.42	0.143	0.140
$\pm 2\sigma_m$ ($n=10$)	0.015	0.023	0.008	0.008	0.09	0.13	0.045	0.044

All data were collected at SDSU from sequence 2 of the same analyses of these standards reported in Table 2.

shown in Table 4) for all of the Zr-doped analyses of the Mo solution standard, the Mo wire standard and UMD-A reported in Table 2. For each standard, the measured $^{97}Mo/^{95}Mo$ and $^{98}Mo/^{95}Mo$ ratios were corrected for mass bias using both simple and external normalization SSB. In every case, the average values and the precisions (either $\pm 2\sigma$ and $\pm 2\sigma_m$) are nearly identical for the data from sequence 1 and sequence 2 (cf., Tables 2 and 6).

The origin of the large difference in precision appears to be related to poorer counting statistics on the $^{91}Zr/^{90}Zr$ ratio for solutions run at high Mo/Zr ratios, and thus, low Zr signal intensities. In order to test this idea, we repeatedly analyzed a series of three Mo solution standards at constant, but different $^{95}Mo/^{90}Zr$ ratios (~1.4, 3.5, and 6.6), and constant signal intensities of Mo ($3.2–3.3 \times 10^{-10}$ V of total Mo). Thus, the signal intensity of Zr decreased over this sequence of analyses. The total number of analyses for each experiment was 7, 9, and 6, respectively. When these data are corrected for instrumental mass bias using simple SSB, the precision is excellent (0.02–0.03‰/AMU, $\pm 2\sigma$). The precision decreases to 0.05–0.12‰/AMU, $\pm 2\sigma$, using external normalization SSB. Thus, the problem is unlikely to lie with the measured Mo isotope ratios. Furthermore, the precision of the analyses corrected using external normalization SSB (either $\pm 2\sigma$ or $\pm 2\sigma_m$) correlates with the Mo/Zr ratio and Zr signal intensity, such that the $\pm 2\sigma$ reproducibility decreases from ± 0.12 to ± 0.06 to ± 0.05‰/AMU as the Mo/Zr ratio of the solution decreases. Finally, this interpretation is consistent with the in-run errors. The average in-run errors for the measured $^{91}Zr/^{90}Zr$ ratio and the Mo isotope ratios corrected for instrumental mass bias using external normalization SSB are ~0.06–0.07‰/AMU ($\pm 2\sigma_m$), which is a factor of ~8–15 higher than the average in-run precision on the measured Mo isotope ratios. Although high Mo/Zr ratios are required in order to reduce matrix effects (Fig. 3), it may be possible to find a combination of Mo/Zr ratio and Mo signal intensity that minimizes matrix effects and maximizes the precision of the Zr isotopic measurement to provide a similar reproducibility for both methods of instrumental mass-bias correction.

Neither the Mo solution standard nor the Mo wire standard can be used to evaluate the accuracy of our techniques. The expected isotopic composition of the Mo wire standard is unknown, but our results suggest that it is ~0.04‰/AMU heavier than the Mo solution standard based on the data corrected using simple SSB. In contrast, the accuracy of our techniques may be determined from the UMD-A standard because it was prepared gravimetrically to give a 1.00‰ increase in its $^{97}Mo/^{95}Mo$ ratio compared to the Mo wire standard from which it was created. This expected result is confirmed by the analyses of UMD-A presented in Table 5, in which the data from Table 2 have been normalized to the Mo wire standard rather than the Mo solution standard. For both methods of correcting for instrumental mass bias, the $\delta^{9X/95}Mo$ values for the replicate analyses of UMD-A are within $\pm 2\sigma_m$ of the expected results. This shows that our mass spectrometric measurements are accurate within the given analytical uncertainties, at least for pure solution standards.

Many studies have demonstrated that isotopic fractionation of heavy elements such as iron, copper, molybdenum or cadmium may occur during their chromatographic separation from a sample (Maréchal et al., 1999; Anbar et al., 2000, 2001; Siebert et al., 2001; Maréchal and Albarède, 2002; Wombacher et al., 2003). This may affect the accuracy of Mo isotopic analyses if the recovery is incomplete. We have not conducted a detailed evaluation of potential Mo isotopic fractionation during our two-column chemistry procedure, which is expected to be <0.1‰/AMU for yields greater than 95% based on the data of Anbar et al. (2001). Instead, the yield of Mo is checked for every sample. For the data presented in Table 2, the recovery varied from 97.7 to 99.5%. Thus, any isotopic fractionation on the column is likely to be significantly less than 0.1‰/AMU. It is important to note that the yields for this study were more stringently controlled than the Mo isotopic data previously published using SSB to correct for the effects of instrumental mass bias (>90% yields; Barling et al., 2001).

Finally, the precision of our techniques can be evaluated using the molybdenite data. The average $\delta^{9X/95}Mo$ values of each molybdenite sample agree within the $\pm 2\sigma_m$ errors for both methods of mass-bias correction. Furthermore, among the data corrected using simple SSB, the solutions containing only Mo show isotopic compositions that are identical to the solutions containing both Mo and Zr within their $\pm 2\sigma_m$ errors (as expected for the averages of replicate analyses). In addition, replicate dissolutions and analyses of two molybdenites (SN and HV) were performed to test the reproducibility of our techniques. In both cases, the average $\delta^{9X/95}Mo$ values of the replicate dissolutions agree within the relatively large $\pm 2\sigma_m$ errors of the data corrected using external normalization SSB. In contrast, the differences of the $\delta^{9X/95}Mo$ values of the replicate dissolutions are generally slightly larger than the $\pm 2\sigma_m$ errors of the data

corrected using simple SSB (maximum differences of 0.04‰/AMU and 0.02‰/AMU for SN and HV, respectively). This suggests an absolute reproducibility of <0.04‰/AMU even if the statistics on replicate analyses of a given sample are better. However, some of the differences between these samples could reflect natural isotopic heterogeneity. In particular, it is important to note that SN-1 and SN-2 (the samples with the larger difference) were sampled from completely different grains in different areas of the specimen. Isotopic heterogeneity for Cu has previously been reported for chalcopyrite grains in a single specimen from the Grasberg igneous Cu–Au deposit (Graham et al., 2004).

Our Mo isotopic data corrected using external normalization SSB are similar in precision (an average value of ±0.14‰/AMU, 2σ, in this study) to previous studies that use this method to correct for instrumental mass bias (e.g., ±0.13‰/AMU, 2σ; Barling et al., 2001). However, as noted previously, simple SSB provides a superior precision (an average value of ±0.04‰/AMU, 2σ, in this study). This is only slightly larger than the precision that can be obtained using the double-spiking method to correct for instrumental mass bias (e.g., ±0.02–0.03‰/AMU, 2σ; Siebert et al., 2001, 2003). Thus, our results suggest that a double-spike may not be necessary in order to obtain high precision Mo isotopic analyses by MC-ICP-MS. However, it is important to note that further study is required to completely validate SSB for silicate mineral and rock samples that, unlike molybdenites and pure Mo solution standards, typically possess a more complex matrix and contain only trace amounts of Mo.

6.2. Mo isotopic composition of molybdenites

Based on the previous discussion, we consider the data corrected for instrumental mass bias using simple SSB to be the most precise and accurate. There appears to be no bias between the samples analyzed with or without Zr, so we use the average of both as the best estimate for the Mo isotopic composition of the molybdenites (Table 2 and Fig. 6). Our results indicate a 0.64‰/AMU range in the Mo isotopic composition of the molybdenites, which is larger than the previous 0.18‰/AMU range reported for such samples (Barling et al., 2001). A plot of $\delta^{97/95}$Mo vs. $\delta^{98/95}$Mo and $\delta^{100/95}$Mo shows that these isotopic variations are mass-dependent (Fig. 6).

The five molybdenites that were analyzed originated in a range of molybdenite-forming hydrothermal environments. Two samples are from porphyry Cu–Mo deposits (HV and Mt. T), and the remaining samples are from a solitary quartz-molybdenite vein from the Sierra Nevada Batholith (SN), a Climax-type deposit (UR-2) and a W–Mo pipe deposit (855111). As shown on Fig. 6, the samples with the lowest $\delta^{97/95}$Mo, $\delta^{98/95}$Mo and $\delta^{100/95}$Mo values are from porphyry Cu–Mo deposits (HV and Mt. T), whereas the two samples with the highest values are from Cu-poor deposits (UR-2 and 855111). The molybdenites from the Sierra Nevada Batholith are intermediate in their Mo isotopic composition. Furthermore, it is important to note that sample 855111 contains the heaviest Mo that was analyzed. Whereas most molybdenite deposits are associated with oxidized granites, sample 855111 is notably associated with a reduced, ilmenite-series two-mica granite (Ishihara and Matsuhisa, 2002). Many factors may have produced the range of the Mo isotopic composition found in these molybdenites, including the $\delta^{97/95}$Mo, $\delta^{98/95}$Mo and $\delta^{100/95}$Mo values inherited from the magma source region, fractionation of Mo isotopes

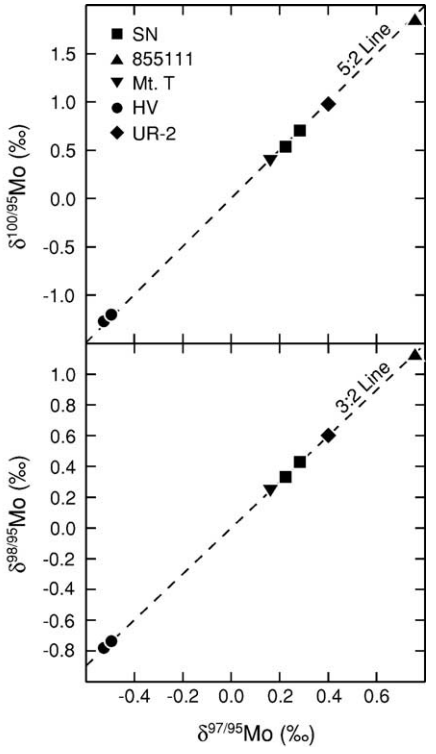

Fig. 6. Mass-dependent Mo isotopic variations for molybdenites. The average values (n=6–10) from Table 2 that were corrected for instrumental mass bias using simple SSB are plotted. All $\delta^{9X/95}$Mo values are expressed relative to the Mo solution standard. The dashed lines represent the expected mass-dependent fractionation lines based on the mass differences between the isotopes used for the ratios on each plot. Error bars based on the $\pm 2\sigma_m$ values of the replicate measurements are smaller than the size of the symbols. Each of these measurements was performed on the Nu Plasma at SDSU.

during processes such as magma devolatilization, or Mo isotopic fractionation during its partitioning between oxide species, such as H_2MoO_4 in the magmatic volatile phase (Candela and Holland, 1984) and molybdenite. More detailed work is required to elucidate the origin of these mass-dependent Mo isotopic variations in molybdenites.

7. Conclusions

Several analytical techniques are currently used to determine mass-dependent molybdenum isotopic variations in natural materials using MC-ICP-MS, including different methods for the separation of Mo from the sample and the correction for instrumental mass bias. In this paper, we have presented a detailed study of the ability of MC-ICP-MS to determine, both precisely and accurately, the isotopic composition of Mo extracted from molybdenite using a low blank, high yield two-column procedure for Mo separation and a simple SSB approach to correct for instrumental mass bias. Based on analyses of molybdenite, the precision of this technique is shown to be similar to published double-spike data (within a factor of ~2). All three of the known matrix effects that might affect the quality of our analyses can be eliminated or controlled. The strongest aspects of the SSB method of correcting for instrumental mass bias (compared to double-spiking) are its greater simplicity and relative insusceptibility to memory effects (e.g., Albarède et al., 2004). However, it is important to note that further study is required to completely validate the standard-sample bracketing method for silicate mineral and rock samples. Analyses of five molybdenites of hydrothermal origin reveal a range in their Mo isotopic composition that is a factor of ~4 greater than the previous range reported for such samples. More detailed work is required to elucidate the origin of these mass-dependent Mo isotopic variations in molybdenites.

Acknowledgments

C. Dalpé and P. Tomascak assisted with the development of our chemical and mass spectrometric techniques. Discussions with M. Horan led to improvements in both the procedural blank and column yield for Mo. G. Helz provided the MQSB-1 standard and helpful ideas for the direction of the project. J. Espino painstakingly entered most of the data presented in this paper into the computer and helped us to discover the higher precision of simple SSB. We thank S. Ishihara for providing sample 855111 for this study. Detailed and constructive reviews from K. Kehm and an anonymous reviewer improved this paper. This research was partially supported by a NASA grant (NAG 54769) to R. Walker and an SDSU Faculty Grant-In-Aid of Research to A. Pietruszka. **[CG]**

References

Albarède, F., Telouk, P., Blichert-Toft, J., Boyet, M., Agranier, A., Nelson, B., 2004. Precise and accurate isotopic measurements using multiple-collector ICPMS. Geochim. Cosmochim. Acta 68, 2725–2744.

Anbar, A.D., Roe, J.E., Barling, J., Nealson, K.H., 2000. Nonbiological fractionation of iron isotopes. Science 288, 126–128.

Anbar, A.D., Knab, K.A., Barling, J., 2001. Precise determination of mass-dependent variations in the isotopic composition of molybdenum using MC-ICPMS. Anal. Chem. 73, 1425–1431.

Arnold, G.L., Weyer, S., Anbar, A.D., 2004. Fe isotope variations in natural materials measured using high mass resolution multiple collector ICPMS. Anal. Chem. 76, 322–327.

Barling, J., Arnold, G.L., Anbar, A.D., 2001. Natural mass-dependent variations in the isotopic composition of molybdenum. Earth Planet. Sci. Lett. 193, 447–457.

Beard, B.L., Johnson, C.M., 1999. High precision iron isotope measurements of terrestrial and lunar materials. Geochim. Cosmochim. Acta 63, 1653–1660.

Beard, B.L., Johnson, C.M., Skulan, J.L., Nealson, K.H., Cox, L., Sun, H., 2003. Application of Fe isotopes to tracing the geochemical and biological cycling of Fe. Chem. Geol. 195, 87–117.

Candela, P.A., Holland, H.D., 1984. The partitioning of copper and molybdenum between silicate melts and aqueous fluids. Geochim. Cosmochim. Acta 48, 373–380.

Carlson, R.W., Hauri, E.H., Alexander, C.M.O'D., 2001. Matrix induced isotopic mass fractionation in the ICP-MS. In: Holland, J.G., Tanner, S.D. (Eds.), Plasma Source Mass Spectrometry: The New Millennium. The Royal Society of Chemistry, Cambridge, pp. 288–297.

Coveney Jr., R.M., Glascock, M.D., 1989. A review of the origins of metal-rich Pennsylvanian black shales, central U.S.A., with an inferred role for basinal brines. Appl. Geochem. 4, 347–367.

Ellis, A.S., Johnson, T.M., Herbel, M.J., Bullen, T.D., 2003. Stable isotope fractionation of selenium by natural microbial consortia. Chem. Geol. 195, 119–129.

Glascock, M.D., Cruse, A.M., Coveney Jr., R.M., 1996. Analysis of metalliferous, organic-rich shales of Pennsylvanian age in the mid-continent. Trans. Am. Nucl. Soc. 74, 120–122.

Graham, S., Pearson, N., Jackson, S., Griffin, W., O'Reilly, S.Y., 2004. Tracing Cu and Fe from source to porphyry: in situ determination of Cu and Fe isotope ratios in sulfides from the Grasberg Cu–Au deposit. Chem. Geol. 207, 147–169.

Halliday, A.N., Lee, D.-C., Christensen, J.N., Rehkämper, M., Yi, W., Luo, X., Hall, C.M., Ballentine, C.J., Pettke, T., Stirling, C., 1998. Applications of multiple collector-ICPMS to cosmochemistry, geochemistry, and paleoceanography. Geochim. Cosmochim. Acta 62, 919–940.

Ishihara, S., Matsuhisa, Y., 2002. Oxygen isotopic constraints on the geneses of the Cretaceous–Paleogene granitoids in the Inner Zone of Southwest Japan. Bull. Geol. Surv. Japan 53, 421–438.

Kehm, K., Hauri, E.H., Alexander, C.M.O'D., Carlson, R.W., 2003. High precision iron isotope measurements of meteoritic

material by cold plasma ICP-MS. Geochim. Cosmochim. Acta 67, 2879–2891.

Maréchal, C., Albarède, F., 2002. Ion-exchange fractionation of copper and zinc isotopes. Geochim. Cosmochim. Acta 66, 1499–1509.

Maréchal, C.N., Télouk, P., Albarède, F., 1999. Precise analysis of copper and zinc isotopic compositions by plasma-source mass spectrometry. Chem. Geol. 156, 251–273.

Matthews, A., Morgans-Bell, H.S., Emmanuel, S., Jenkyns, H.C., Erel, Y., Halicz, L., 2004. Controls on iron-isotope fractionation in organic-rich sediments (Kimmeridge Clay, Upper Jurassic, southern England). Geochim. Cosmochim. Acta 68, 3107–3123.

McManus, J., Nägler, T.F., Siebert, C., Wheat, C.G., Hammond, D.E., 2002. Oceanic molybdenum isotopic fractionation: diagenesis and hydrothermal ridge-flank alteration. Geochem. Geophys. Geosyst. 3, doi:10.1029/2002GC000356.

Nägler, T.F., Siebert, C., Lüschen, H., Böttcher, M.E., 2005. Sedimentary Mo isotope record across the Holocene fresh–brackish water transition of the Black Sea. Chem. Geol. 219, 283–295.

Pietruszka, A.J., Carlson, R.W., Hauri, E.H., 2002. Precise and accurate measurement of ^{226}Ra–^{230}Th–^{238}U disequilibria in volcanic rocks using plasma ionization multicollector mass spectrometry. Chem. Geol. 188, 171–191.

Rehkämper, M., Frank, M., Hein, J.R., Porcelli, D., Halliday, A., Ingri, J., Liebetrau, V., 2002. Thallium isotope variations in seawater and hydrogenetic, diagenetic, and hydrothermal ferromanganese deposits. Earth Planet. Sci. Lett. 197, 65–81.

Rouxel, O., Ludden, J., Carignan, J., Marin, L., Fouquet, Y., 2002. Natural variations of Se isotopic composition determined by hydride generation multiple collector inductively coupled plasma mass spectrometry. Geochim. Cosmochim. Acta 66, 3191–3199.

Rouxel, O., Ludden, J., Fouquet, Y., 2003. Antimony isotope variations in natural systems and implications for their use as geochemical tracers. Chem. Geol. 200, 25–40.

Russell, W.A., Papanastassiou, D.A., Tombrello, T.A., 1978. Ca isotope fractionation on the Earth and other solar system materials. Geochim. Cosmochim. Acta 42, 1075–1090.

Siebert, C., Nägler, T.F., Kramers, J.D., 2001. Determination of molybdenum isotope fractionation by double-spike multicollector inductively coupled plasma mass spectrometry. Geochem. Geophys. Geosyst. 2, doi:10.1029/2000GC000124.

Siebert, C., Nägler, T.F., von Blanckenburg, F., Kramers, J.D., 2003. Molybdenum isotope records as a potential new proxy for paleoceanography. Earth Planet. Sci. Lett. 211, 159–171.

Siebert, C., Kramers, J.D., Meisel, T., Morel, P., Nägler, T.F., 2005. PGE, Re–Os, and Mo isotope systematics in Archean and early Proterozoic sedimentary systems as proxies for redox conditions of the early Earth. Geochim. Cosmochim. Acta 69, 1787–1801.

Walczyk, T., von Blanckenburg, F., 2002. Natural iron isotope variations in human blood. Science 295, 2065–2066.

Wombacher, F., Rehkämper, M., Mezger, K., Münker, C., 2003. Stable isotope compositions of cadmium in geological materials and meteorites determined by multiple-collector ICPMS. Geochim. Cosmochim. Acta 67, 4639–4654.

Zhu, X.K., O'Nions, R.K., Gao, Y., Reynolds, B.C., 2000a. Secular variation of iron isotopes in North Atlantic deep water. Science 287, 2000–2002.

Zhu, X.K., O'Nions, R.K., Guo, Y., Belshaw, N.S., Rickard, D., 2000b. Determination of natural Cu-isotope variation by plasma-source mass spectrometry: implications for use as geochemical tracers. Chem. Geol. 163, 139–149.